Journal of Biomedical Optics

SPIEDigitalLibrary.org/jbo

Epithelium and Bowman's layer thickness and light scatter in keratoconic cornea evaluated using ultrahigh resolution optical coherence tomography

Rahul Yadav
Ranjini Kottaiyan
Kamran Ahmad
Geunyoung Yoon

SPIE

Epithelium and Bowman's layer thickness and light scatter in keratoconic cornea evaluated using ultrahigh resolution optical coherence tomography

Rahul Yadav,[a] Ranjini Kottaiyan,[b] Kamran Ahmad,[c] and Geunyoung Yoon[a,b,c]
[a]University of Rochester, The Institute of Optics, 275 Hutchinson Road, Rochester, New York 14627
[b]University of Rochester, Flaum Eye Institute, 210 Crittenden Boulevard, Rochester, New York 14642
[c]University of Rochester, Center for Visual Science, 274 Meliora Hall, Rochester, New York 14627

Abstract. A custom-developed ultrahigh resolution optical coherence tomography with an axial resolution of 1.1 μm in corneal tissue was used to characterize thickness and light scatter of the epithelium and Bowman's layer in keratoconic (KC) cornea noninvasively. A 4-mm wide vertical corneal section around the apex in nine KC and eight normal eyes was imaged *in vivo*. The epithelium and Bowman's layer were visualized and their thickness profiles were quantified. Scatter was quantified based on the sensitivity normalized mean signal intensity distribution. Average mean thickness of the epithelium and Bowman's layer in KC eyes was significantly smaller ($p < 0.05$) than the normal eyes. The epithelium thickness variation across a central 3-mm cornea was significantly larger in KC eyes than in normal eyes. The scatter in KC eyes was significantly increased only for Bowman's layer. The changes observed in this study could improve our understanding of the underlying disease mechanism of KC and can provide new indications for early disease diagnosis. [DOI: 10.1117/1.JBO.17.11.116010]

Keywords: optical coherence tomography; keratoconus; corneal epithelium; Bowman's layer.

Paper 12490 received Jul. 31, 2012; revised manuscript received Oct. 9, 2012; accepted for publication Oct. 10, 2012; published online Nov. 1, 2012.

1 Introduction

Keratoconus (KC) is a degenerative disorder of the eye where the cornea assumes a conical shape due to noninflammatory thinning and steepening of the central and/or para-central cornea.[1,2] The change in corneal shape leads to the induction of significant amounts of higher order aberrations in the eye, resulting in marked decrease in the optical quality of the eye.[1] One in 2000 individuals in the general population is affected by this disorder.[3] Although the thinning of the stroma in KC eyes, particularly at the apex of the cone, has been well characterized,[2] the effect of the disease on other corneal layers is still under investigation, due mainly to the inability to image the thin corneal layers. Previous studies on KC eyes have shown epithelial thinning,[4–8] and incursion of fine cellular processes in the Bowman's layer[9] along with structural abnormalities and sharply edged defects.[10,11] Most of these changes in KC eyes have been observed *ex-vivo*, limited primarily to corneal buttons obtained after penetrating keratoplasty was performed on subjects with advanced KC. The capability to measure these changes *in vivo* in patients with different disease severity will provide us with a more comprehensive understanding of the underlying disease pathogenesis and a method to objectively assess the disease progression. Hence there is a scientific interest in studying these changes *in vivo*.

Recent studies have investigated corneal epithelium thickness profile in KC eyes *in vivo* using very high frequency ultrasound[6] and optical coherence tomography (OCT).[7,8] Central epithelium thinning[6–8] and donut pattern in the thickness profile[6] were observed in these *in vivo* studies. *In vivo* confocal microscope (IVCM) which provides cellular level resolution en face images of the cornea has also been commonly used in studying KC corneas.[12,13] Previous studies using IVCM have shown changes in the density of epithelial cells[13,14] and stromal keratocytes[14,15] in KC corneas. Increased haze/scatter in all the corneal layers[13,16] has also been observed in the KC eyes. These findings suggest that any change in corneal microstructure will disrupt its transparency, increasing light scatter. Therefore, we measured backscatter in OCT as an indirect indicator of abnormal biological changes.

OCT is capable of providing two-dimensional (2-D) cross-sectional or three-dimensional (3-D) volumetric images of the cornea covering a larger lateral field. However, commercially available anterior segment OCT systems lack sufficient axial resolution to visualize and quantify thin corneal layers. Hence we used an ultrahigh resolution OCT,[17] which has an axial resolution of 1.1 μm in corneal tissue and is capable of visualizing individual corneal layers over a large field. The goal of this study is to characterize the thickness and light scatter of corneal epithelium and Bowman's layer in the KC eyes using the ultrahigh resolution OCT.

2 Methods

2.1 *Subject Recruitment and Assessment*

Eight patients (nine eyes) diagnosed with KC at the Department of Ophthalmology, University of Rochester Strong Memorial Hospital were recruited for the study. Since using fellow eyes

Address all correspondence to: Geunyoung Yoon, University of Rochester Eye Institute, 601 Elmwood Avenue, Box 314 Rochester, New York 14642. Tel: 585-273-4998; Fax: 585-276-2432; E-mail: yoon@cvs.rochester.edu

0091-3286/2012/$25.00 © 2012 SPIE

of patients for a study can lead to inaccuracy in statistical variance if the two eyes have similar disease severity,[18,19] only one eye of all the patients was used for the study, except for one KC patient whose both eyes were included in the study as the severity of the disease in the two eyes was considerably different. Eight eyes of eight age-matched normal subjects with no history of ocular surgery, no prior or current ocular disease besides refractive error served as controls. The research adhered to the tenets of the Declaration of Helsinki. The protocol was approved by the Research Subjects Review Board at the University of Rochester. Informed consent was obtained from all participants after the purpose of the study and the procedures were explained. Corneal topography and keratometry values of all the eyes were obtained using a combined slit-scanning elevation topography and placido disc system (Orbscan II; Bausch & Lomb Surgical, Rochester, NY). Keratometry readings have traditionally been used as the indicator of disease severity and classifying KC into mild, moderate and severe KC.[20] However, in our study there was an overlap in the keratometry readings of mild KC and normal patients. We decided to use corneal coma, the most dominant aberration in the KC eyes as a measure of the disease severity.[21–23] The corneal aberrations were calculated from the corneal elevation maps obtained by the topography data. The severity of KC was assessed based on the root mean square (RMS) of the horizontal and vertical corneal coma over a 4-mm pupil. The clinical measures for the subjects are shown in Table 1.

2.2 *Ultrahigh-Resolution Spectral Domain OCT*

A custom-built ultrahigh resolution OCT was used to visualize and quantify individual corneal layers *in vivo* over a 4 mm wide vertical corneal section around the apex. The OCT system achieved an axial resolution of 1.1 μm in corneal tissue by using broadband light (Bandwidth: 375 nm, Spectral range: 625 to 1000 nm) of a supercontinuum light source (Leukos SM 20).[24] The OCT was built in free space to avoid reduction in axial resolution due to dispersion induced by the optical fiber[25–27] and because a fiber optic directional coupler was not available for such a broad bandwidth light source. The beam was split equally into reference and sample arm using a 50/50 cube beamsplitter. Dispersion was matched between sample and reference arm by using identical optics in both the arms.

In the detection arm, a custom designed spectrometer based on a modified Czerny-Turner configuration was used.[28] As a dispersive element a diffraction grating (500 grooves/mm) was used. To remove astigmatism, the dominating aberration present in Czerny Turner spectrometer designs, an astigmatism correcting cylindrical lens was placed just before the linescan camera. This spectrometer achieves a spectral resolution of better than 0.15 nm over the 625 to 1000 nm spectral range, thus achieving an imaging depth of about 1 mm.[29] The details on the design considerations for the OCT system are provided elsewhere.[17]

The power of the light shined into the eye was 0.75 mW, which is 80 times below the maximum permissible exposure as dictated by the American National Standards Institute (ANSI).[30] The linescan camera exposure time of 1 ms was used and each image frame consisted of 250 A-scans. Approximately 100 B-scans at the frame rate of 2 frames/s were obtained at the same scan location. Best frames with no or minimum motion artifacts were then selected for image processing and data analysis. A bite-bar was used to minimize patient head movement.

2.3 *Outcome Measures*

Central epithelial thinning[4–8] and irregular thinning and breaks in Bowman's layer along with incursion of fine cellular processes in the Bowman's layer[9–11] and increased haze in epithelium and Bowman's layer[13,16] have been observed in previous studies on KC corneas. Therefore, the outcome measures for this study include the differences in the average thickness, thickness variability and the amount of light scatter of the normal and KC eyes along the superior-inferior sections for these two layers. Here light scatter was used as a measure for the structural modifications, for example due to cellular incursions in the epithelium and Bowman's layer.

2.4 *Image Analysis*

Image analysis was carried out using custom-developed Matlab based software (Fig. 1). The first step was to obtain surface profiles of epithelium and Bowman's layer in each of the images. The procedure for surface profile generation started with manual selection of 11 different points on the interface of each layer by the user. These data points were then spline interpolated to generate an initial estimate of each interface in the image. Subsequently, around the initial estimate, the algorithm searched for the pixels with highest signal intensity in a region of ± 5 pixels for the tear-epithelium interface and ± 10 pixels for the epithelium-Bowman's layer interface and the Bowman's layer-stroma interface. The region to search for anterior epithelial layer was kept smaller to avoid bias from the tear-air interface. The peak

Table 1 Patient characteristics.

	Keratoconus (range) ($n = 9$)	Normals (range) ($n = 8$)
Age (years)	40.5 ± 13.3 (24–58)	37.1 ± 13.3 (25–55)
Corneal Astigmatism (D)	4.6 ± 2.6 (0.2–9.4)	1.3 ± 0.6 (0.4–2.4)
Max K (D)	53.0 ± 7.0 (45.4–65.5)	45.1 ± 2.0 (41.9–47.9)
Min K (D)	48.4 ± 5.7 (40.2–57.5)	43.8 ± 2.1 (40.8–46.4)
Corneal Coma (μm)	1.2 ± 0.75 (0.3–3.4)	0.2 ± 0.1 (0.1–0.3)
Central corneal thickness (μm)	443.2 ± 32.4 (406.4–487.2)	511.2 ± 36.4 (462.2–546.5)

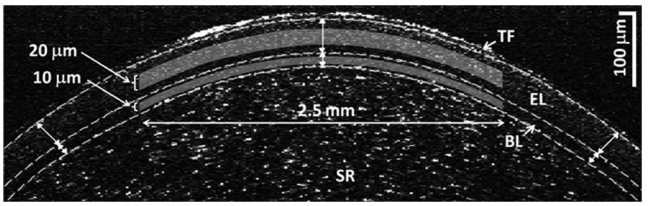

Fig. 1 OCT image analysis. Corneal image obtained by the OCT system showing the ocular surface. TF: Tear film, EL: Epithelium, BL: Bowman's layer, SR: Stroma. The white dashed curves indicate the identified interfaces of the epithelium and Bowman's layer. Thickness profiles were obtained by measuring radial distances as shown by the arrows. Sensitivity normalized signal intensity averaged over a region 2.5 mm wide and of thickness of 20 μm and 10 μm, respectively, shown in shaded gray, in epithelium and Bowman's layer was used to measure light scatter. See Fig. 2(a) for an unannotated version of the same image.

intensity pixels were then fitted with a fifth order polynomial to obtain the final interface profile. Refractive distortion correction was carried out on the profiles using ray tracing.[31] From the distortion corrected surface profiles, the thickness profile of the epithelium and Bowman's layer were quantified by measuring the thickness along the radial direction at each corneal position. For both the estimation of physical thickness and refractive distortion correction, the refractive index of 1.401 for the epithelium[32] and an average corneal refractive index of 1.376 for Bowman's layer[33] were assumed for normal as well as KC corneas at the OCT source wavelength. Thickness variability was evaluated by calculating the standard deviation of thickness profile.

For evaluating the light scatter in biological tissue using OCT images, mean of the OCT signal intensity corresponding to backward scatter can be used.[34] However, since the sensitivity of the OCT system reduces when the relative distance between the sample and the reference mirror location is increased, a sample when placed at a position closer relative to the reference mirror location appears brighter than when it is positioned a little further. To correct for this variation, the signal intensity was normalized by the experimentally measured axial position dependent sensitivity of the OCT system. The axial position dependent sensitivity was obtained by replacing the sample with a mirror and moving it axially to measure axial PSFs of the OCT system while the reference mirror was kept stationary. The peak values for the obtained PSFs at seven axial locations from 0 to 1.1 mm were then interpolated using the spline function to create a continuous function representing the axial depth dependent sensitivity. The intensity values in each A-scan from real cornea were divided by this function to obtain sensitivity normalized signal intensities.[17] The light scatter was then quantified as the mean of the sensitivity normalized signal intensity values in a region of 2.5 mm width and optical thickness (refractive index $\times$ physical thickness) of 20 μm and 10 μm in the center of the epithelium and Bowman's layer, respectively. Paired t-test was performed to examine statistical significance ($p < 0.05$) in the outcome measures between the groups.

3 Results

3.1 *OCT Imaging*

Representative corneal images obtained with the system for a normal [Fig. 2(a)] and three KC patients [Fig. 2(b)–2(d)] with increasing disease severity demonstrated the feasibility of the OCT to visualize the epithelium and Bowman's layer in both groups. Qualitatively, it can be seen that in KC patients, the thickness of both epithelium and Bowman's layer is smaller than in the normal subject. An increase in the amount of backscatter in both the layers can also be observed. Interestingly, in the most severe KC [Fig. 2(d)], the overall OCT signal from the cornea is relatively weaker than other patients. The reduction could be attributed to the considerably increased steepness of the corneal curvature which causes increased reflection power loss of incoming OCT beam at the interface. Also, in the most severe KC, the interface of the Bowman's layer with epithelium and stroma is difficult to distinguish. In two of the nine KC eyes measured in this study, the Bowman's layer could not be visualized. In such eyes the entire thickness from the tear film to the stroma was assumed to be epithelium and these eyes were excluded in our analysis on the Bowman's layer.

3.2 *Thickness*

Mean $\pm$ standard deviation of the average thickness across the epithelial layer was found to be 45.2 ± 7.5 μm in KC and 51.6 ± 3.8 μm in normal eyes, with the difference in thickness between the two groups being statistically significant. Similarly, the Bowman's layer in KC eyes was significantly thinner (13.1 ± 2.1 μm) than normal eyes (16.7 ± 2.6 μm). The

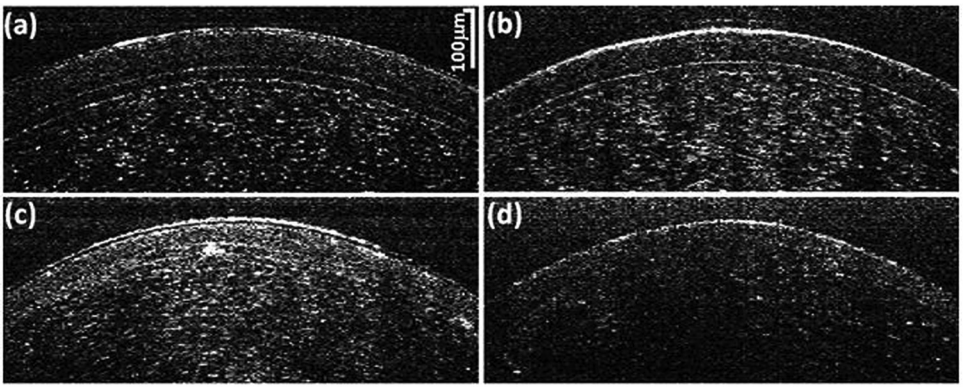

Fig. 2 Images obtained by the system for a normal (a), three KC patients (b), (c) and (d) with increasing corneal coma, where corneal coma represents the KC disease severity. A reduction in the epithelium and Bowman's layer thickness can be seen for KC eyes. In most severe KC patient (d) the interfaces of Bowman's layer with epithelium and stroma are difficult to distinguish. Hyper-reflective centers, visible as white patches, can be seen in the Bowman's layer of the moderate KC (c).

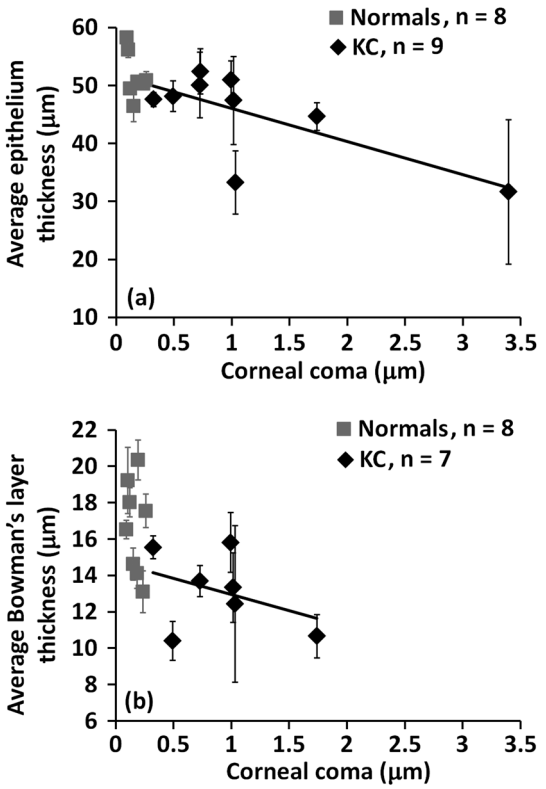

Fig. 3 Scatter plot showing mean epithelium (a) and Bowman's layer (b) thickness plotted against corneal coma (4 mm pupil size). The epithelium and Bowman's layer thickness in KC eyes was significantly smaller than normal eyes ($p = 0.023$ for epithelium and $p = 0.006$ for Bowman's layer). A negative correlation was observed between epithelium thickness and disease severity ($R^2 = 0.50$) while no correlation was found for Bowman's layer thickness ($R^2 = 0.15$).

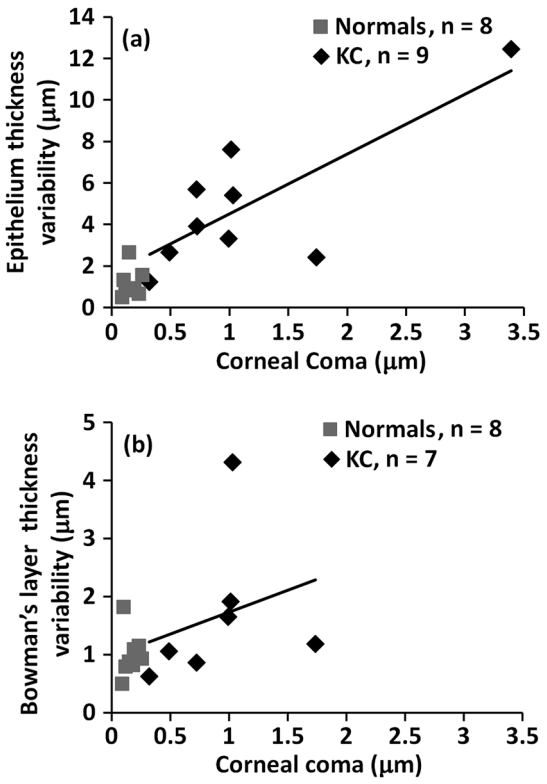

Fig. 4 Scatter plot showing epithelium (a) and Bowman's layer (b) thickness variability plotted against corneal coma (4 mm pupil size). The thickness variability was significantly higher in epithelium ($p = 0.004$) but not in Bowman's layer ($p = 0.090$). A positive correlation can be observed between disease severity and epithelium thickness variability ($R^2 = 0.61$), while no correlation was observed for Bowman's layer ($R^2 = 0.08$).

epithelium and Bowman's layer thicknesses were plotted against corneal coma, to examine their correlation with disease severity. For the KC group, a negative correlation was found between both the average epithelium thickness and corneal coma ($R^2 = 0.50$) [Fig. 3(a)] and average Bowman's layer thickness and corneal coma ($R^2 = 0.15$) [Fig. 3(b)]. No correlation was found for the normal group.

3.3 *Thickness Variability*

The thickness variability was significantly higher in KC eyes for epithelium (5.0 ± 3.4 μm in KC and 1.1 ± 0.7 μm in normal eyes), but did not differ for the Bowman's layer (1.7 ± 1.3 μm in KC and 1.0 ± 0.4 μm in normal eyes). The thickness variability increased with severity of KC for epithelium ($R^2 = 0.61$) [Fig. 4(a)] while for the Bowman's layer no such trend was observed ($R^2 = 0.08$) [Fig. 4(b)].

Figure 5 shows characteristic thickness profiles of the two layers across the ± 1.5 mm lateral distance from the apex along the superior-inferior direction. To take the effect of the disease severity into account, the KC group of nine eyes was divided into two groups, KC group 1 and KC group 2, consisting of five and four eyes, respectively, using an arbitrary threshold criterion of 1 μm corneal coma. The thickness of the epithelium in the normal group showed almost no changes over the 3 mm diameter cornea [Fig. 5(a)]. In both the KC groups, the epithelial thickness of inferior cornea including around apex was smaller than the superior region however, statistical significance was found only for KC group 2 [Fig. 5(a)]. For the Bowman's layer, no characteristic pattern in the thickness profile was observed for both normal and KC groups [Fig. 5(b)].

3.4 *Light Scatter*

Light scatter in the epithelium averaged over all subjects in the KC and normal eyes was 28.7 ± 13.5 and 22.5 ± 7.1 in arbitrary units (linear scale), respectively [Fig. 6(a)]. However, this increase in scatter for KC eyes was statistically insignificant. For the Bowman's layer, the two eyes where Bowman's layer could not be visualized were excluded from the analysis. The scatter in the KC eyes was also larger than the normals with the values of 31.6 ± 16.1 in KC and 20.1 ± 4.7 in normal eyes [Fig. 6(b)]. This difference was statistically significant although no correlation was observed with disease severity.

4 Discussion

Our custom-developed OCT was capable of visualizing the epithelium and Bowman's layer in detail in both the KC and normal eyes *in vivo*, which enabled us to precisely characterize the two thin layers in both the groups and study the differences. A 4-mm wide vertical corneal section around the apex was imaged. Since the cone is a protrusion in the KC cornea, the cone location in the KC eye should be same as the corneal apex. Our findings hence are based on the data from around

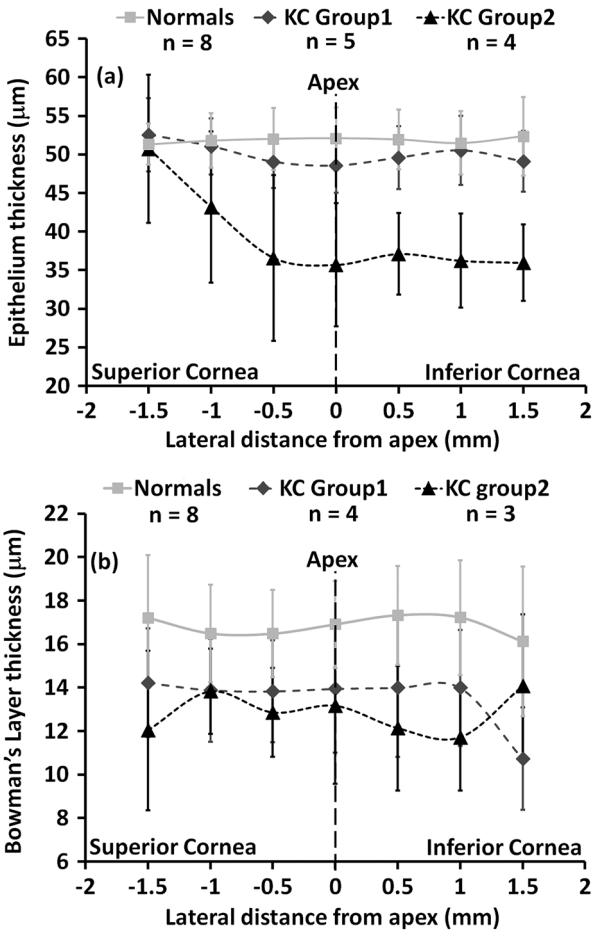

Fig. 5 The plot showing average local epithelial thickness (a) and Bowman's layer thickness (b), averaged over the subjects, as a function of the lateral distance from the apex for normals and two KC groups. KC group 1 has eyes with corneal coma (4 mm pupil) <1 μm while KC group 2 eyes have corneal coma >1 μm. A pattern of inferior epithelial thinning was found in both the KC groups with the inferior thinning being significantly larger in KC group 2. The epithelial thickness in the inferior cornea was significantly smaller than the superior cornea only for KC group 2 ($p = 0.001$). No specific pattern was observed in the Bowman's layer thickness profile for all the groups.

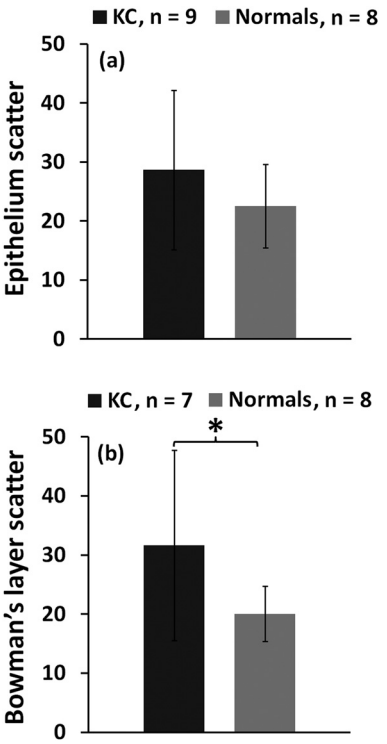

Fig. 6 Bar graph comparing scatter in epithelium (a) and Bowman's layer (b) for normal and KC eyes. The increase in scatter was statistically significant ($p = 0.036$) only for the Bowman's layer.

the cone. We expect that the trends found in the present study would become less dominant in corneal areas further away from the cone.

Average thickness of both epithelium and Bowman's layer over a 4 mm cross-section around the apex of the cone was significantly reduced for KC eyes. This is consistent with the previous observation of central epithelial thinning using histopathology,[4,5] very high frequency digital ultrasound arc scanner[6] and *in vivo* OCT[7,8] and irregular thinning of Bowman's layer using *ex-vivo* scanning electron microscopy.[9,11] Moreover in the present study, we further investigated the impact of disease severity on the corneal layers represented by corneal coma, the most dominant higher order aberration present in the KC eyes.[21] The epithelium thickness showed a negative correlation ($R^2 = 0.50$) with the KC severity [Fig. 3(a)] while no correlation was observed for the Bowman's layer thickness [Fig. 3(b)].

The increase in the variability of the thickness profile of epithelium over the central 4 mm of the KC corneas was significant compared to the normal group. A positive correlation between the corneal coma and epithelium thickness variability was observed ($R^2 = 0.61$) [Fig. 4(a)]. In both KC groups, we also found a pattern in the epithelium thickness profile around the apex that the epithelium thickness along the inferior cornea from the apex was reduced in comparison to the superior cornea [Fig. 5(a)]. However, statistical significance was only found in the severe KC group where corneal coma >1 μm. Our hypothesis to explain this finding of inferior thinning in epithelium is as follows. It has been suggested that corneal epithelium may modify itself to compensate for corneal surface distortions and maintain a spherical anterior corneal surface.[6] KC leads to the bulging of the cornea towards the inferior side. Thus, the inferior thinning of the epithelium occurs to compensate for this inferior stromal bulging so that the deviations of the corneal surface from a smooth spherical profile can be minimized. Further investigation using a wider field of OCT imaging in a larger sample size is required to confirm this hypothesis.

The very high frequency digital ultrasound arc scanner study[6] observed a donut ring pattern in the KC epithelium thickness profile with thinning in the center and thickening in the periphery. This pattern, however, was observed over a wider lateral zone (10 mm in diameter) compared to the present study. It will be interesting to examine if a wider field OCT images the same pattern at the peripheral cornea.

The correlation between Bowman's layer thickness variability and corneal coma was insignificant ($R^2 = 0.08$). No specific trend was found in the thickness profile of the Bowman's layer for both KC and normal eyes. Irregular thinning of the Bowman's layer has been observed in previous histopathological studies,[11] which suggests that there should be an increase in the thickness variability of Bowman's layer for KC eyes. In the current study increased Bowman's layer thickness variability was

found but this increase was statistically insignificant. It should be noted in Fig. 4(b) that one of the KC patients has significantly higher Bowman's layer thickness variability than normals, suggesting that on increasing the sample size of the study an increase in thickness variability in Bowman's layer may be found.

Scatter in the epithelium and Bowman's layer was quantified as the mean of axial sensitivity normalized OCT intensity signals. A significant increase in the scatter was observed only in the Bowman's layer for the KC patients. The axial sensitivity was measured experimentally by replacing the sample with a flat mirror. However, we cannot rule out other potential contributions including intensity variation due to strong specular reflection around the apex of the cone and speckle. This increased backscatter in Bowman's layer was previously found as the increased haze in the IVCM measurements in the KC cornea.[16] With the increase in backscatter for Bowman's layer it also becomes increasingly difficult to distinguish its boundary with the epithelium and stroma. This observation is consistent with the previous histopathological observation of cellular incursions of epithelial and stromal cells into the Bowman's layer.[9] Two KC eyes in our study did not show a clear Bowman's layer and were excluded from this analysis.

Clinical interest in exploring new methods to allow for detection of subclinical KC has been increasingly growing as this ability is critical in corneal refractive surgery to avoid development of post-operative ectasia.[35,36] It may also provide opportunity to at least halt disease progression using therapeutic interventions such as corneal collagen crosslinking[37] before KC develops further and causes severe degradation in visual function. We found a correlation between disease severity and epithelium thickness and thickness variability, and also discovered a trend in the epithelium thickness profile. It would be important to investigate whether such subtle structural differences in corneal layers could be used to screen KC suspects.

5 Conclusion

We have demonstrated structural differences in the epithelium and Bowman's layer of the normal and KC cornea using an ultrahigh resolution OCT. These structural differences can be useful in improving our understanding of the consequences and the underlying mechanisms of the disease and may provide new metrics for early diagnosis of the disease.

Acknowledgments

This research was supported by grants from NIH/NEI EY014999, RPB and Core Grant P30 EY007125.

References

1. J. H. Krachmer, R. S. Feder, and M. W. Belin, "Keratoconus and related non-inflammatory corneal disorders," *Surv. Ophthalmol.* **28**(4), 293–322 (1984).
2. Y. S. Rabinowitz, "Keratoconus," *Surv. Ophthalmol.* **42**(4), 297–319 (1998).
3. H. Hofstetter, "A keratoscopic survey of 13,395 eyes," *Am. J. Optom. Acad. Optom.* **36**(1), 3–11 (1959).
4. M. W. Scroggs and A. D. Proia, "Histopathological variation in keratoconus," *Cornea* **11**(6), 553–559 (1992).
5. K. Tsubota et al., "Corneal epithelium in keratoconus," *Cornea* **14**(1), 77–83 (1995).
6. D. Z. Reinstein, T. J. Archer, and M. Gobbe, "Corneal epithelium thickness profile in the diagnosis of keratoconus," *J. Refract. Surg.* **25**(7), 604–610 (2009).
7. S. Haque, T. Simpson, and L. Jones, "Corneal and epithelial thickness in keratoconus: a comparison of ultrasonic pachymetry, orbscan II, and optical coherence tomography," *J. Refract. Surg.* **22**(5), 486–493 (2006).
8. Y. Li et al., "Corneal epithelial thickness mapping by Fourier-domain optical coherence, tomography in normal and keratoconic eyes," *Ophthalmology* (e-published ahead of print) (2012).
9. T. Sherwin et al., "Cellular incursion into Bowman's membrane in the peripheral cone of the keratoconic cornea," *Exp. Eye Res.* **74**(4), 473–482 (2002).
10. A. J. Tuori et al., "The immunohistochemical composition of corneal basement membrane in keratoconus," *Curr. Eye Res.* **16**(8), 792–801 (1997).
11. S. Sawaguchi et al., "Three-dimensional scanning electron microscopic study of keratoconus corneas," *Arch. Ophthalmol.* **116**(1), 62–68 (1998).
12. R. L. Niederer et al., "Laser scanning *in vivo* confocal microscopy reveals reduced innervation and reduction in cell density in all layers of the keratoconic cornea," *Invest. Ophthalmol. Vis. Sci.* **49**(7), 2964–2970 (2008).
13. M. C. Mocan et al., "In vivo confocal microscopy for the evaluation of corneal microstructure in keratoconus," *Curr. Eye Res.* **33**(11–12), 933–939 (2008).
14. J. C. Erie et al., "Keratocyte density in keratoconus. A confocal microscopy study," *Am. J. Ophthalmol.* **134**(5), 689–695 (2002).
15. J. Y. F. Ku et al., "Laser scanning *in vivo* confocal analysis of keratocyte density in keratoconus," *Ophthalmology* **115**(5), 845–850 (2008).
16. N. Effron and J. G. Hollingsworth, "New perspective on keratoconus as revealed by corneal confocal microscopy," *Clin. Exp. Optom.* **91**(1), 34–55 (2008).
17. R. Yadav et al., "Micrometer axial resolution OCT for corneal imaging," *Biomed. Opt. Ex.* **2**(11), 3037–3046 (2011).
18. F. Ederer, "Shall we count numbers of eyes or numbers of subjects?," *Arch. Ophthalmol.* **89**(1), 1–2 (1973).
19. J. Katz, "Two eyes or one? The data analyst's dilemma," *Ophthalmol. Surg.* **19**(8), 585–589 (1988).
20. K. Zadnik et al., "Biomicroscopic signs and disease severity in keratoconus: collaborative longitudinal evaluation of keratoconus (CLEK) study group," *Cornea* **15**(2), 139–146 (1996).
21. N. Maeda et al., "Wavefront aberrations measured with hartmann-shack sensor in patients with keratoconus," *Ophthalmol.* **109**(11), 1996–2003 (2002).
22. M. Gobbe and M. Guillon, "Corneal wavefront aberration measurements to detect keratoconus patients," *Cont. Lens Anterior Eye* **28**(2), 57–66 (2005).
23. J. L. Alió and M. H. Shabayek, "Corneal higher order aberrations: a method to grade keratoconus," *J. Refract. Surg.* **22**(6), 549–545 (2006).
24. W. Drexler, "Ultrahigh-resolution optical coherence tomography," *J. Biomed. Opt.* **9**(1), 47–74 (2004).
25. W. Drexler et al., "Investigation of dispersion effects in ocular media by multiple wavelength partial coherence interferometry," *Exp. Eye Res.* **66**(1), 25–33 (1998).
26. C. K. Hitzenberger, A. Baumgartner, and A. F. Fercher, "Dispersion induced multiple signal peak splitting in partial coherence interferometry," *Opt. Commun.* **154**(4), 179–185 (1998).
27. C. K. Hitzenberger et al., "Dispersion effects in partial coherence interferometry: implications for intraocular ranging," *J. Biomed. Opt.* **4**(1), 144–151 (1999).
28. K. S. Lee, K. P. Thompson, and J. P. Rolland, "Broadband astigmatism-corrected Czerny-Turner spectrometer," *Opt. Express* **18**(22), 23378–23384 (2010).
29. R. Leitgeb et al., "Ultrahigh resolution Fourier domain optical coherence tomography," *Opt. Express* **12**(10), 2156–2165 (2004).
30. A.N.S.I., "Z136.1 Safe use of lasers," Laser Institute of America (2007)
31. A. Podoleanu et al., "Correction of distortions on optical coherence tomography imaging of the eye," *Phys. Med. Biol.* **49**(7), 1277–1294 (2004).

32. S. Patel, J. Marshall, and F. W. Fitzke, "Refractive index of the human corneal epithelium and stroma," *J. Refract. Surg.* **11**(2), 100–105 (1995).
33. D. A. Atchison and G. Smith, *Optics of the Human Eye*, pp. 11–20, Butterworth-Heinemann, Edinburgh, UK (2000).
34. A. F. Fercher et al., "Measurement of intraocular distances by backscattering spectral interferometry," *Opt. Commun.* **117**(1–2), 43–48 (1995).
35. T. Seiler and A. W. Quurke, "Iatrogenic keratectasia after LASIK in a case of forme fruste keratoconus," *J. Cataract Refract. Surg.* **24**(7), 1007–1009 (1998).
36. J. B. Randleman et al., "Risk assessment for ectasia after corneal refractive surgery," *Ophthalmol.* **115**(1), 37–50 (2008).
37. G. Wollensak, "Crosslinking treatment of progressive keratoconus: new hope," *Curr. Opin. Ophthalmol.* **17**(4), 356–360 (2006).